IN SITU X-RAY PROBES FOR PIEZOELECTRICITY IN EPITAXIAL FERROELECTRIC CAPACITORS

DAL-HYUN DO [a]; ALEXEI GRIGORIEV [a]; DONG MIN KIM [a]; CHANG-BEOM EOM [a]; PAUL G. EVANS [a]; ERIC M. DUFRESNE [a]

[a] Department of Materials Science and Engineering, University of Wisconsin, Madison, WI, U.S.A.

Online Publication Date: 01 January 2008

PLEASE SCROLL DOWN FOR ARTICLE

Taylor & Francis
Taylor & Francis Group

In Situ X-Ray Probes for Piezoelectricity in Epitaxial Ferroelectric Capacitors

Dal-Hyun Do,[1] Alexei Grigoriev,[1] Dong Min Kim,[1] Chang-Beom Eom,[1] Paul G. Evans,[1,*] and Eric M. Dufresne[2]

[1]Department of Materials Science and Engineering, University of Wisconsin, Madison, WI 53706, U.S.A.
[2]Advanced Photon Source, Argonne National Laboratory, Argonne, IL 60439, U.S.A.

ABSTRACT

Probing the piezoelectricity and ferroelectricity of thin film devices and nanostructures quantitatively has proven to be challenging because the appropriate experimental tools have had a limited range of usefulness. We show here that the piezoelectric and ferroelectric properties of epitaxial thin films can be measured quantitatively using time-resolved synchrotron x-ray microdiffraction. Microdiffraction combines structural specificity with the appropriate spatial resolution and ability to probe structures with electrical contacts. Our measurements of piezoelectric coefficients and coercive electric fields for $Pb(Zr,Ti)O_3$ capacitors using this approach are in excellent quantitative agreement with results obtained electrically and mechanically. The time and spatial resolution of microdiffraction probes are well-defined and decoupled from electrical and mechanical resonances of the ferroelectric capacitor.

INTRODUCTION

Observing and manipulating the degrees of freedom of complex oxide materials forms the basis for a range of scientific and technological advances, ranging from multifunctional materials to piezoelectric nanostructures [1, 2]. In ferroelectrics, the strain and electrical polarization are related through piezoelectricity. The mechanisms responsible for piezoelectricity in all but the simplest materials and devices involve the interplay of mechanical, electrical, and

compositional effects that are the objects of continuing research [3, 4]. In relaxor ferroelectrics, an electric field can alter the symmetry of the solid between rhombohedral and tetragonal, resulting in a large enhancement of the piezoelectric response [4]. In nanostructures of tetragonal materials such as $Pb(Zr,Ti)O_3$, an understanding of the role of ferroelectric domains is rapidly being developed [3]. Quantitatively describing the structural response of ferroelectrics to electric fields, however, is a problem that is at the limits of conventional experimental techniques. The benefits of a new probe for piezoelectricity at the nanoscale can be as simple as the correlation of different techniques for measuring piezoelectric coefficients, but can extend to deeper questions of the connection of the response of complex oxides to external fields.

X-ray diffraction is widely used to investigate polarization switching, phase transitions, and piezoelectricity in ferroelectric materials under static or quasi-static conditions [5−8]. X-ray studies of piezoelectricity make use of the piezoelectric deformation of the lattice and the resulting shift of Bragg reflections in reciprocal space. Polarization switching can be probed using an effect connecting the lack of inversion symmetry to a difference in the intensity of reflections from domains of opposite polarizations [6, 9]. The absorption lengths of hard x-rays in complex oxide ferroelectrics, and in oxide electrodes such as $SrRuO_3$ (SRO), are long compared to the film thicknesses. Diffraction experiments can thus be conducted *in situ* on operating devices. This use of continuous well-defined electrodes allows measurements under homogeneous electric field conditions. Here, we use the electric field dependence of the lattice constant of an epitaxial ferroelectric to extract piezoelectric and ferroelectric quantities, including the piezoelectric coefficient and the coercive electric field.

EXPERIMENTAL

The ferroelectric thin film capacitors for these experiments were formed from a (001)-oriented tetragonal $Pb(Zr_{0.45}Ti_{0.55})O_3$ (PZT) thin film with a thickness of 400 nm. The PZT layer was deposited onto uniform epitaxially grown SRO bottom electrode on a $SrTiO_3$ (001) substrate [10]. Polycrystalline 200 μm-diameter SRO top electrodes were formed on the PZT layer using a shadow mask, and annealed under an oxygen atmosphere at 500°C for 30 min. In electrical measurements, voltage pulses were applied to the bottom electrode of the capacitor, with the top electrode grounded.

X-ray experiments used synchrotron x-ray microdiffraction techniques at station 7ID-C of the Advanced Photon Source of Argonne National Laboratory. A monochromatic incident beam of 10 keV x-rays was focused to a spot with a 400 nm full width at half maximum using Fresnel zone plate optics [11]. Focusing the beam in this way allows devices with lithographic features or small dimensions to be probed. Changes in the c-axis spacing of the PZT thin film were measured in the diffraction experiments with a sensitivity to changes

in the c-axis lattice constant of approximately $\Delta c/c \sim 10^{-5}$ using the (002) Bragg x-ray reflection.

The diffracted x-ray beam was collected by an avalanche photodiode (APD) detector, which allowed x-ray count rates up to several million photons per second. A multichannel scaler recorded the time dependence of the intensity of the diffracted beam by accumulating counts from the APD in bins with 10 or 20 μs dwell times. The time-dependent evolution of the lattice constants of the PZT thin film capacitors during voltage pulses was followed using radial reciprocal space scans through the PZT (002) Bragg reflection. At each angular step in the scan, the intensity of the Bragg reflection was measured as a function of time during a series of 18 identical voltage pulses. The intensities from equivalent times within the pulses were summed to improve the counting statistics. The diffraction data presented here was acquired in regions near the center of the top electrodes of the PZT capacitors.

RESULTS AND DISCUSSION

The longitudinal piezoelectric response of the PZT thin film causes a lattice distortion along the surface normal, and shifts the PZT (002) reflection in reciprocal space, which results in lower or higher Bragg angles in diffraction experiments. The direction of the shift depends on the relative polarities of the applied electric field and the remnant polarization; when the electric field is parallel to the polarization vector the unit cell expands. Similarly, the unit cell contracts when the polarization vector and electric field are in opposite directions. Large electric fields in the direction opposite to the built-in polarization can switch the direction of the polarization. Repeated pulses of electric fields of either polarization will thus switch the polarization, with the first pulse, and subsequently result only in lattice expansion.

The expansion of the lattice in response to a series of electric field pulses of each polarization is shown in Fig. 1. The distortion of the lattice was observed in measurements of intensity of the PZT (002) x-ray reflection as a function of time and the 2θ angle of a θ-2θ scan during 500 μs-duration voltage pulses. There were large shifts in the PZT (002) toward lower values of 2θ, and hence larger lattice constants during both positive and negative 10 V voltage pulses. The lattice parameter was constant before and after the voltage pulses, and identical in states with opposite polarizations.

The coercive electric fields of these films corresponded to voltages smaller than the 10 V amplitude of the voltage pulses. The Bragg peak thus shifts to lower 2θ angle during electric field pulses because the polarization and electric field are parallel after the first pulse, regardless of the polarity of the voltage. The maximum change in the Bragg angle occurred at the maximum electric field.

The data shown in Fig. 1 can be used to find the change in the c-axis lattice constant of the PZT thin films relative to the zero-field state as a function of

(a)   (b)
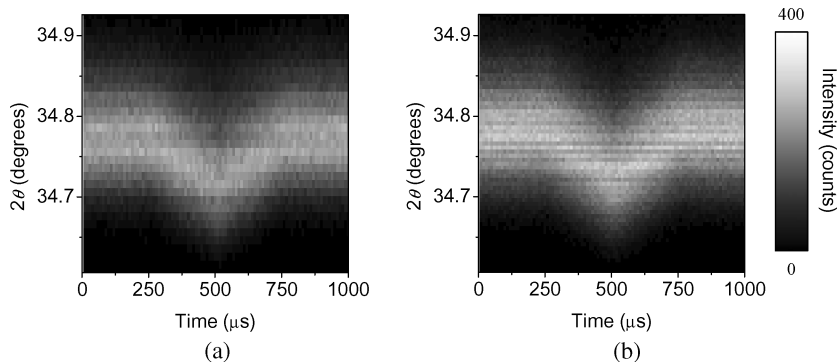
Figure 1. Intensity near the PZT (002) Bragg x-ray reflection as a function of θ-2θ and time during (a) positive and (b) negative 10 V triangular voltage pulses with 500 μs duration beginning at 250 μs. The intensity difference between (a) and (b) is due to the lack of inversion symmetry in PZT.

the applied voltage. The change in c-axis lattice constant was proportional to the applied voltage, as shown for this case in Fig. 2. The maximum change in the lattice constant was 0.55 pm at the maximum of both positive and negative voltage pulses, which corresponds to 0.13% strain. The longitudinal piezoelectric coefficient d_{33} is

$$d_{33} = \left(\frac{\partial S_3}{\partial E_3} \right),$$
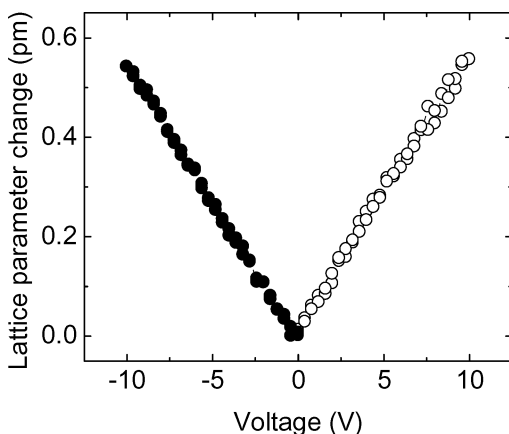
Figure 2. The change in the c-axis lattice parameter of the PZT thin film as a function of applied voltage. Open and closed circles are measured with positive and negative voltages, respectively.

where S_3 is the strain and E_3 is the electric field in the direction of the remnant polarization. Based on the measurements in Fig. 2, the longitudinal piezo-electric coefficients for positive and negative pulses were 53 and 54 pm V^{-1}, respectively. At these modest strains there is no departure from the linearity in the piezoelectric response.

When the voltage pulses alternate in polarity, the remnant polarization can be switched if the pulses reach amplitudes higher than voltages corresponding to the coercive electric field. The response of the lattice of PZT thin films to triangular voltage pulses of alternating polarity with 2000 μs duration and ± 10 V amplitude are shown in Fig. 3(a). At the start of the voltage pulse the polarization vector and the applied electric field are in opposite directions. As the amplitude of the applied voltage increases, the PZT (002) Bragg reflection initially shifts to higher angle as the c-axis lattice constant of the PZT thin film decreases. At the coercive voltage, the remnant polarization begins to switch and eventually reaches the opposite polarization state. A sudden lattice expan-sion accompanies switching and the x-ray reflection abruptly shifts to a lower Bragg angle. After reaching its full extension at the maximum positive voltage $+10$ V, the lattice parameter contracts linearly to its 0 V value. The same series of phenomena, consisting of the sequence of contraction, switching, expan-sion, and finally contraction to the zero-field lattice constant, also occurs in the subsequent negative half-cycle of the voltage pulse. A difference in intensity between the two remnant polarization states arising from the noncentrosym-metric unit cell of PZT is visible as a change in the intensity of the diffracted beam at the times corresponding to switching in Fig. 3(a) [6, 12].

The shift of the x-ray reflection during the bipolar voltage pulse can be used quantitatively to produce an electromechanical hysteresis loop. Fig. 3(b) shows the change in the lattice parameter of the PZT thin films as a function of the applied voltage. For each of the two polarization states, the lattice constant was proportional to the applied field in the range of voltages extending from the peak voltage of one polarity to the coercive electric field of the opposite polarity. The coercive voltages in Fig. 3(b) are within 1 V of voltages determined using polarization-electric field hysteresis loops. The mechanical hysteresis loop in Fig. 3(b) slightly asymmetric and was shifted in towards positive voltages. Such asymmetry is often due to the contribution of polarization domains that have not completely switched in response to the voltage pulses [13]. The same effect can shift the hysteresis loop along the voltage axis due to an effective internal bias and lower the piezoelectric constants, both of which are also apparent in Fig. 3(b).

The piezoelectric coefficients in the linear regions of the piezoelectric hysteresis shown in Fig. 3(b) were 42 and 45 pm V^{-1}, respectively, for the polarization states produced by positive and negative voltage pulses. These slightly smaller piezoelectric coefficients than those measured using electrical pulses of only one polarity (Fig. 2) further confirm the incomplete switching of a small fraction of polarization domains. Piezoelectric coefficients measured
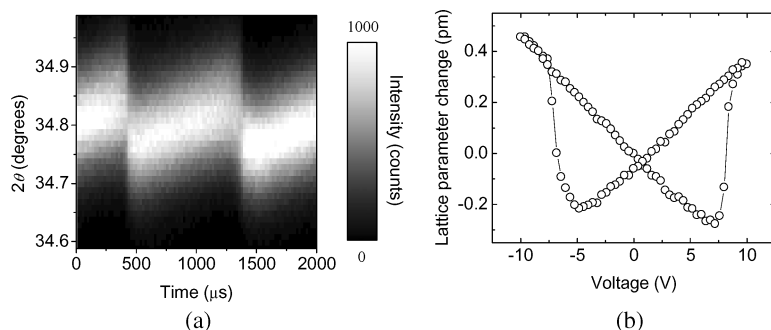
Figure 3. (a) Intensity near the PZT (002) Bragg reflection as a function of θ-2θ and time during a bipolar voltage pulse of consisting of two triangular voltage pulses. The complete voltage cycle had a duration of 2000 μs and amplitude of 20 V peak-to-peak. (b) The electromechanical hysteresis loop derived from the time dependence of the 2θ angle of the PZT (002) x-ray reflection.

mechanically in similar single-crystal PZT thin films span a range of values, from 50 to 200 pm V^{-1} depending on the composition and orientation of PZT film [14]. The piezoelectric response of ferroelectric thin films is also reduced by the mechanical constraints imposed by a relatively thick substrate.

CONCLUSION

Structural phenomena in these relatively uncomplicated tetragonal PZT thin films ferroelectrics are one example of the broad range of questions that can be addressed using new probes. In the future, we anticipate that contributions of individual domains within structurally complex thin films to the total piezo-electric response can be unraveled using structural probes. When both 90° and 180° domain walls are present within the film, or if separate domains of tetragonal and rhombohedral phases coexist, the structural problems become more complex, but can be addressed by this approach. Piezoelectric force mi-croscopy (PFM) can do the same for domains near the surface with excellent spatial resolution [15, 16]. Some uncertainty in the interaction between the tip and surface and the need for calibration with standards can pose important problems in PFM techniques, however. These are areas in which a complemen-tary structural probe may have a role [17].

Finally, transverse piezoelectric coefficients, which lead to distortions in the plane perpendicular to the applied electric field, can also be probed by observing x-ray reflections with a component of the scattering wave vector in the plane of the film. A small, highly intense focused x-ray beam should make it possible to study piezoelectric nanostructures as thin as a few unit

cells and of arbitrarily small lateral dimensions. Other future directions can be enabled by making use of the unique capabilities of synchrotron radiation. X-rays from synchrotron sources are bunched into short pulses on the order of 100 ps or less. By taking advantage of these short pulses, the approach we demonstrate here has been adapted to the shorter timescales relevant to the propagation of domain walls during polarization switching [18]. X-ray scattering can also simultaneously probe other degrees of freedom within the sample using magnetic scattering processes. With magnetic scattering, x-ray techniques can similarly address the magnetism and structure of multiferroic complex oxides.

REFERENCES

1. N. A. Spaldin and M. Fiebig, *Science* **309**, 391 (2005).
2. Z. L. Wang and J. H. Song, *Science* **312**, 242 (2006).
3. Z. Ma, F. Zavaliche, L. Chen, J. Ouyang, J. Melngailis, A. L. Roytburd, V. Vaithyanathan, D. G. Schlom, T. Zhao, and R. Ramesh, *Appl. Phys. Lett.* **87**, 072907 (2005).
4. S.-E. Park and T. R. Shrout, *J. Appl. Phys.* **82**, 1804 (1997).
5. D. L. Marasco, A. Kazimirov, M. J. Bedzyk, T.-L. Lee, S. K. Streiffer, O. Auciello, and G.-R. Bai, *Appl. Phys. Lett.* **79**, 515 (2001).
6. D.-H. Do, P. G. Evans, E. D. Isaacs, D. M. Kim, C.-B. Eom, and E. M. Dufresne, *Nature Mater.* **3**, 365 (2004).
7. B. Noheda, J. A. Gonzalo, L. E. Cross, R. Guo, S.-E. Park, D. E. Cox, and G. Shirane, *Phys. Rev. B* **61**, 8687 (2000).
8. R. Bolt, J. Albertsson, G. Svensson, K. Stahl, and J. C. Hanson, *J. Appl. Cryst.* **30**, 383 (1997).
9. R. W. James, *The Optical Principles of X-ray Diffraction*, Ithaca, N. Y., Cornell University Press (1965), p. 33.
10. C. B. Eom, R. B. Van Dover, J. M. Phillips, D. J. Werder, J. H. Marshall, C. H. Chen, R. J. Cava, R. M. Fleming, and D. K. Fork, *Appl. Phys. Lett.* **63**, 2570 (1993).
11. Z. Cai, B. Lai, Y. Xiao, and S. Xu, *J. de Physique IV* **104**, 17 (2003).

12. V. V. Antipov, A. A. Blistanov, E. D. Roshchupkina, R. Tucoulou, L. Ortega, and D. V. Roshchupkin, *Appl. Phys. Lett.* **85**, 5325 (2004).
13. W. Ma and D. Hesse, *Appl. Phys. Lett.* **84**, 2871 (2004).
14. L. Chen, V. Nagarajan, R. Ramesh, and A. L. Roytburd, *J. Appl. Phys.* **94**, 5147 (2003).
15. A. L. Kholkin, Ch. Wütchrich, D. V. Taylor, and N. Setter, *Rev. Sci. Instrum.* **67**, 1935 (1996).
16. C. Durkan, D. P. Chu, P. Migliorato, and M. E. Welland, *Appl. Phys. Lett.* **76**, 366 (2000).
17. S. Hong, H. Shin, J. Woo, and K. No, *Appl. Phys. Lett.* **80**, 1453 (2002).
18. A. Grigoriev, D.-H. Do, D. M. Kim, C. B. Eom, B. Adams, E. M. Dufresne, and P. G. Evans, *Phys. Rev. Lett.* **96**, 187601 (2006).